https://doi.org/10.5194/hess-2022-57
Preprint. Discussion started: 16 February 2022

Hydrology and Earth System Sciences
Open Access
EGU
Discussions

Quantitative effects of antecedent effective rainfall on *ID* threshold for debris flow

Shaojie Zhang [1], Hongjuan Yang [1], Dunlong Liu [2], Kaiheng Hu[1], Fangqiang Wei[1]

1. Key Laboratory of Mountain Hazards and Earth Surface Process, Institute of Mountain Hazards and Environment, Chinese Academy of Sciences, Chengdu 610041, China

2.College of Software Engineering, Chengdu University of Information and Technology, Chengdu, 610225, China

Correspondence to: K.H. Hu, E-mail: khhu@imde.ac.cn, F.Q. Wei, E-mail: fqwei@imde.ac.cn

Abstract

Studies have shown that the antecedent effect precipitation (*AEP*) is closely related to rainfall intensity-duration (ID) threshold of debris flow. However, the quantitative relationship between the *AEP* and ID threshold is still undetermined. In this study, a hydrological process based numerical model (Dens-ID) that can derive the ID threshold curve is adopted to address this issue. Jiangjia Gully (JJG) in Dongchuan District of Yunnan Province was chosen as the study area, Dens-ID was used to derive a series of ID threshold curves corresponding to different *AEP*. Based on calculated data sets including *AEP*, ID curves, parameters of ID curve equation (α and β), and debris flow density, the influence of *AEP* on the ID threshold curve is deeply explored. We found that although solid materials and runoff are the two necessary conditions for the formation of debris flow, the specific roles played in which are different: the volume of loose solid sources provides a basal condition for debris flow and determines the scale of debris flow, while the runoff volume will have a sudden change during the rainfall process, which is a key factor promoting the formation of debris flow. In the condition of *AEP* ranging from 20 mm to 90 mm, *AEP* and α can

https://doi.org/10.5194/hess-2022-57
Preprint. Discussion started: 16 February 2022

Hydrology and Earth System Sciences
Discussions
Open Access

be described by the equation α=-0.0078AEP^2+0.68AEP+6.43, and β shows a linear change law with *AEP*. The error of the two equations were evaluated using 45 historical rainfall data that triggered debris flows, which is equal to 37.85% and 11.1%. Due to the two functions, the ID threshold curve can regularly move in the I-D coordinate system rather than a conventional threshold curve stay the same regardless of *AEP* variation, it is beneficial to improve the prediction capacity of the ID threshold.

1 Introduction

Precipitation that affects debris flow formation includes triggering rainfall and antecedent effective precipitation (AEP) before the event (Chen et al., 2015; Chen et al., 2018; Oorthuis et al., 2021). AEP is precipitation that remains in soil before a debris flow occurs; it reflects the degree of soil saturation (Zhang et al., 2015). Increased AEP, and thus increased moisture content, has been shown to enhance surface rainfall-induced runoff in various environments (Tisdall, 1951; Luk, 1985; Le Bissonnais et al., 1995; Castillo et al., 2003; Jones et al., 2017). Additionally, the increased soil water content caused by AEP decreases the shear strength of the loose soil mass in a debris flow gully, enhancing the supply rate of the solid material required for debris flow formation (Lehmann and Or, 2012; Kim et al., 2013; Ruette et al., 2014). AEP has an important effect on the rainfall threshold for triggering debris flow. Debris flow prediction can be improved by quantifying this effect (Chen et al., 2018; Zhao et al., 2019; Hirschberg et al., 2021; Marino et al., 2020; Jiang et al., 2021).

A rainfall threshold is generally a fixed value of some rainfall parameter such as cumulative rainfall, hourly rainfall intensity, or AEP (Marra et al., 2017); alternatively, it can be a curve of two rainfall parameters (Peres and Cancelliere, 2014), such as the rainfall intensity–rainfall

https://doi.org/10.5194/hess-2022-57
Preprint. Discussion started: 16 February 2022

Hydrology and Earth System Sciences
Discussions

duration threshold curve (Cain, 1980) and rainfall intensity–antecedent rainfall curve (Long et al., 2020). The most commonly investigated threshold is the intensity (I) versus duration (D) curve (Crosta and Frattini, 2003; Cannon et al., 2008; Guzzetti et al., 2008; Berti et al., 2020), which has the form $I=\alpha D^{\beta}$, where I represents the average rain intensity in the rainfall process that triggers debris flow, D represents the rainfall duration, and α and β are empirical parameters. Segoni et al. (2018) analyzed the rainfall thresholds of landslides and debris flows reported in 107 articles and found that the threshold model based on the *ID* threshold curve accounted for the highest proportion, approximately 48.6%. Empirical and process-based methods are commonly used to derive the *ID* threshold curves of debris flow (Segoni et al., 2018). The empirical model workflow is as follows. Data on debris flow events and the associated rainfall in a target area are collected, and the I and D values of each rainfall process that triggered a debris flow event are calculated. D and I are plotted on the x and y axes, respectively, and the *ID* threshold curve is fitted using these data. As for the process-based methods, a typical physical parameter (P_i) that can represent debris flow occurrence in a gully is first chosen, and the change in this parameter has a certain threshold interval (e.g., [P_{low}, P_{upper}]). During a rainfall process, P_i changes because of hydrological processes such as rainfall infiltration and runoff. When it falls into the interval [P_{low}, P_{upper}], a debris flow may be triggered under these rainfall conditions. Then a numerical model is built to calculate P_i by inputting different rainfall conditions characterized by different D and I. For a certain value of P_i (e.g., P_{upper}), the [D_i, I_i] data for which the calculated value is equal to P_{upper} are collected during model calculations. These collected data are then used to fit the threshold curves (Long et al., 2020). Papa et al. (2013) proposed that the total area (S) of shallow landslides induced by rainfall in a gully plays an important role in debris flow formation. Therefore, the ratio

https://doi.org/10.5194/hess-2022-57
Preprint. Discussion started: 16 February 2022

of S to the catchment area is used as the threshold (that is, P_i), and the TRIGERS model (Baum et al., 2002, 2008) and a rainfall scenario simulation are adopted to calculate P_i and search for the combination of all [I_i, D_i] at which the P_i calculated by the model is equal to a preset value. Next, the *ID* threshold curve corresponding to this value is obtained by fitting. Although shallow landslides induced by rainfall in a basin are very important for debris flow formation, the effect of hydrodynamic conditions provided by rainfall-induced runoff on debris flow formation cannot be ignored. Scholars have argued that a water-soil mixture in a gully can be formed by coupling between the rainfall-induced solid material and runoff (Church and Jakob, 2020). The debris flow density represents the fluid characteristics of the mixture and can be used to incorporate the two major factors (rainfall-induced loose solid material and rainfall-induced runoff) that affect debris flow formation into numerical simulation models (Zhang et al., 2020; Long et al., 2020). A numerical model (Dens-ID) is used to correlate rainfall parameters with the density boundaries of 1.2 and 2.2 g/cm^3; the *ID* threshold curve of debris flow can then be constructed in the physical framework. The *ID* curve fitted by this model reportedly has a shape similar to that of the statistics-based curve. The precision of debris flow prediction by this model in Jiangjia Gully (JJG) in Yunnan Province, China, is approximately 80.5%, which is 27.7% higher than that of the statistics-based *ID* curve (Zhang et al., 2020).

It is difficult to introduce AEP as a dependent variable into the power function $I = \alpha D^{\beta}$. Attempts to analyze the effect of AEP on the parameters α and β have resulted in the following consensus. A larger AEP can decrease the rainfall conditions triggering debris flow: however, an equation that describes the quantitative evolution of each parameter (α or β) with AEP has not been derived. Some studies have used the relationship between daily rainfall and antecedent

https://doi.org/10.5194/hess-2022-57
Preprint. Discussion started: 16 February 2022

rainfall (Kim et al., 1991; Glade et al., 2000; Dahal and Hasegawa, 2008; Giannecchini et al., 2012) or a combination of daily rainfall intensity and rainfall duration (Hasnawir and Kubota, 2008; Khan et al., 2012; Zhao et al., 2019; Kim et al., 2020; Yang et al., 2020) to investigate the effects of AEP on the rainfall threshold. Jiang et al. (2021) investigated the probabilistic rainfall thresholds for debris flows after the Wenchuan earthquake and found that antecedent precipitation plays an important role in long-duration rainfall-induced debris flows. Zhao et al. (2019) introduced the simulated antecedent soil moisture into a probabilistic threshold and found that it exhibited better prediction performance than the daily rainfall intensity and rainfall duration (*ED*) threshold. However, all of these studies lack a quantitative description of the effect of AEP on the rainfall threshold. This lack is attributed mainly to the absence of sufficient historical data including AEP, rainfall intensity, rainfall duration, and debris flow events, which makes it difficult to conduct differential analysis and to derive a function that quantitatively describes their relationship.

To quantify the effect of AEP on the *ID* threshold curve, JJG in Yunnan Province, China, was chosen as the study area, and the Dens-ID numerical model was used to build its *ID* threshold curve database. The mechanism by which AEP affects the *ID* threshold curve is thoroughly discussed using this database, and equations for the functions describing the relationships between AEP and the parameters α and β were derived through data analysis.

2 Methods

2.1 Dens-ID

Shallow landslides and bed erosion are the two main sources of debris flow material; both

https://doi.org/10.5194/hess-2022-57
Preprint. Discussion started: 16 February 2022

may be present in the same gully, but one type is always dominant (Gabet and Mudd, 2006; Berti and Simoni, 2005; Coe et al., 2008; Long et al., 2020). Debris flow gullies with shallow landslides as the source of solid materials are widely distributed in southwestern China (Zhang et al., 2020). Dens-ID focuses on landslide-dominated supply and is designed to derive the *ID* threshold curves of debris flow by calculating the debris flow density in rainfall scenario simulations. The key function of this model is to correlate debris flow density with rainfall parameters, as described by Zhang et al. (2020) and Long et al. (2020). Debris flows are complex mixtures of water, fragmented rock, and sediments of all sizes (Chmiel et al., 2020). Dens-ID simplifies this complex nonuniform flow (Iverson, 1997) as a water-soil mixture. The runoff amount [$V_w(t)$] and amount of solid material [$V_s(t)$] are taken as the two parameters contributing to debris flow formation. Using these two parameters as the inputs of Eq. 1, Dens-ID can calculate the density of the water-soil mixture.

$$\rho_{mix}(t) = \frac{\rho_w V_w(t) + \rho_s V_s(t)}{V_{mix}(t)} \tag{1}$$

where $\rho_{mix}(t)$ is the density of the water-soil mixture, ρ_w is the water density, ρ_s is the density of soil particles, and $V_{mix}(t)$ is the volume of the water-soil mixture, which is the sum of $V_w(t)$ and $V_s(t)$. $V_w(t)$ and $V_s(t)$ are the key variables for correlating the debris flow density with the rainfall parameters, which can be derived by pixel-based hydrological simulation (Long et al., 2020).

Based on a digital elevation model (DEM) of a debris flow gully, Dens-ID uses the theory of runoff generation from excess precipitation to control the infiltration boundary in the topsoil (Zhang et al., 2014a). It then simulates the vertical water movement within the soil mass using the differential equation of Richards (1931).

https://doi.org/10.5194/hess-2022-57
Preprint. Discussion started: 16 February 2022

Hydrology and Earth System Sciences Discussions

Governing equation of infiltration border: $-D(\theta)\frac{\partial\theta}{\partial z}+K(\theta)=I(t)$ (2)

Richards' differential equation: $\frac{\partial\theta}{\partial t}=\frac{\partial}{\partial z}[D(\theta)\frac{\partial\theta}{\partial z}]]-\frac{\partial K(\theta)}{\partial\theta}$ (3)

where θ is the soil water content; $D(\theta)=K(\theta)/(d\theta/d\psi)$ is the soil water diffusivity; z is the soil depth, which is positive downward along the soil depth, taking the topsoil as the origin; $K(\theta)$ is the hydraulic conductivity; $I(t)$ is the rainfall intensity; and ψ is the soil matric suction.

After the hydrological simulation, Dens-ID outputs the water soil content θ (i, t), soil matric suction $\psi(i, t)$, and runoff depth $dw(i, t)$ for each pixel of the DEM. Dens-ID then calculates $V_w(t)$ using the runoff depth $dw(i, t)$, as shown in Eq. 4.

$$V_w(t) = \sum_{t=1}^{T}\sum_{i=1}^{n} S_g * dw(i,t) \quad (4)$$

where n represents the total number of grid cells that can generate runoff at time t, and $V_w(t)$ represents the total volume of runoff in a gully at time t. Using $\theta(i, t)$ and $\psi(i, t)$ as inputs, Dens-ID adopts an infinite slope model (Zhang et al., 2014b; Liu et al., 2016; Zhang et al., 2018) to calculate the unstable depth of each grid cell $ds(j,t)$. It then calculates $V_s(t)$ using $ds(j, t)$, as shown in Eq. 5.

$$V_s(t) = \sum_{t=1}^{T}\sum_{j=1}^{m} S_g * ds(j,t) \quad (5)$$

where m represents the number of grid cells that can provide solid material at time t, and $V_s(t)$ is the total volume of solid material in the gully at time t.

The mixture density can be derived by substituting various rainfall parameters, including rainfall intensity (I) and rainfall duration (D), into the right side of Eq. 2. Then Dens-ID can correlate the rainfall parameters with the debris flow density.

2.2 Derivation of *ID* threshold curve using Dens-ID

https://doi.org/10.5194/hess-2022-57
Preprint. Discussion started: 16 February 2022

The debris flow density varies between 1.2 and 2.3 g/cm^3. The values within the interval [1.2, 2.3] represent a density set. In nature, a debris flow with a density ρ_{mix} cann be triggered by high-intensity or long-duration rainfall. Inputting rainfall scenarios with different combinations of [I_i, D_i] into Dens-ID makes it possible to simulate debris flow initiation by rainfall in nature. Using a given density value (ρ_{mix}) during the calculation, Dens-ID collects all the [I_i, D_i] data that meet the conditions of the rainfall scenarios (Fig. 1). That is, when the selected [Ii, Di] are used as input, the output of the model is equal to ρ_{mix}. The collected [I_i, D_i] values represent another data group, which is referred to as a rainfall parameter set. Each data point [I_i, D_i] corresponds to a unique value of ρ_{mix} within the density set; thus, the correlation between the rainfall parameters and debris flow density can then be established by Dens-ID. An *ID* curve can then be fitted through the collected [I_i, D_i] data to show the relationship between *I* and *D*. Each fitted *ID* curve corresponds to a unique ρ_{mix} within the density set, which is also considered to be the isodensity line (Zhang et al., 2020). Two values close to the left and right boundaries are chosen from the density set as ρ_{mix}, and the *ID* threshold curve corresponding to these two density values can represent the lower and upper boundaries for debris flow formation. The *ID* curves corresponding to a density value ρ_{mix} are fitted as follows:

Step 1: Assign values of 1.2 and 2.2 g/cm^3 to ρ_{mix}.

Step 2: Assign a value to the AEP. In nature, the AEP represents the antecedent soil moisture before the rainfall process that may trigger a debris flow. In Dens-ID, the natural debris flow gully is divided into a series of grid cells, and the AEP represents the soil moisture content of each grid cell before rainfall infiltration. Using the initial hydrological conditions represented by the AEP, Dens-ID simulates hydrological processes such as runoff and infiltration during the triggering

Hydrology and Earth System Sciences
Open Access
Discussions

precipitation process. To quantitatively analyze the effect of AEP on the *ID* threshold curve, AEP_i was assigned values of 10, 20, 30, 40, 50, 60, 70, 80, 90, 100, 110, and 120 mm.

Step 3: Assign a value to I_i, which generally represents the average rainfall intensity of a rainfall process that can trigger a debris flow and is held constant until the calculations in Step 4 are complete. The initial value of I_i is set to 1 mm/h. When Step 4 is complete, I_i is increased by 0.5 up to $I_{\max}$. At $I_{\max}$, a debris flow with density ρ_{mix} can be triggered in the gully when $D = 1$.

Step 4: Under constant I_i, the calculation time of the model starts at $t = 1$ h and increases by 1 h at each calculation step until $t = D_i$, where D_i represents the rainfall duration required to trigger a debris flow with density ρ_{mix}. After $t = D_i$, the model calculation for a given I_i is complete.

Step 5: Repeat Steps 3 and 4 and collect the I_i and D_i values at which Dens-ID outputs the pre-set ρ_{mix}. When the rainfall intensity I_i increases to $I_{\max}$, the calculation for a given AEP_i is complete. Thus, the data set of I_i and D_i for a certain AEP_i is obtained, and the corresponding *ID* threshold curve can be fitted using these data.

Step 6: Repeat Steps 2, 3, 4, and 5, and collect the I_i and D_i values. When AEP reaches 120 mm, the calculation for a given ρ_{mix} is complete.

https://doi.org/10.5194/hess-2022-57
Preprint. Discussion started: 16 February 2022

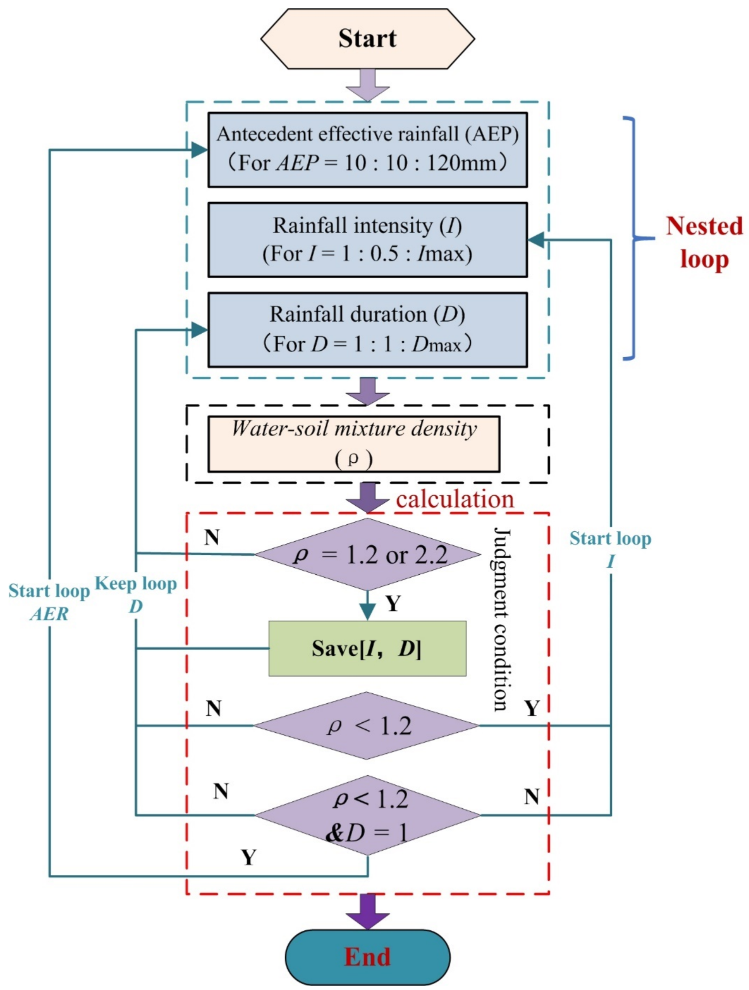

Fig. 1 Flow chart of model calculation for obtaining [I_i, D_i] data

3 Study area and data collection

3.1 Jiangjia Gully

JJG is located in the Dongchuan district of Kunming City, Yunnan Province, China, and is the primary tributary of the Xiaojiang River. JJG has a drainage area of 48.6 km^2, and its elevation ranges from 1040 to 3260 m (Fig. 2). The terrain in JJG is steep; the relative relief between the ridge and valley is approximately 500 m, and most slopes have a gradient exceeding 25°. Menqian and Duozhao gullies, which are shown in Fig. 2, are the two main tributaries and account for 64.7% of the entire drainage area. These two tributaries constitute the initiation zones of debris flow in JJG, and their channels are typically narrow and V-shaped [Fig. 3(c)]. JJG is characterized by intense tectonism, and approximately 80% of the exposed rocks are highly fractured and slightly metamorphosed. The predominant sandstone and slate can be easily identified by their light and dark colors, respectively. Both rock types are weak and easily weathered and fragmented (Yang et al., 2020).

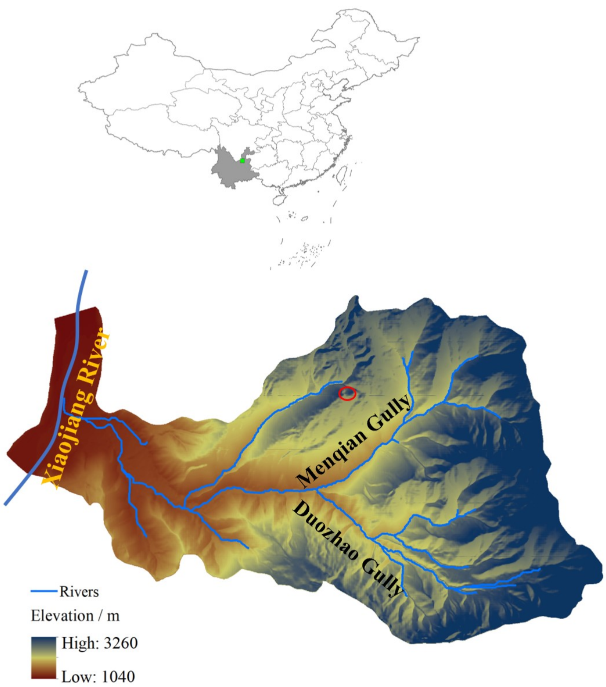

Fig. 2 Location of JJG

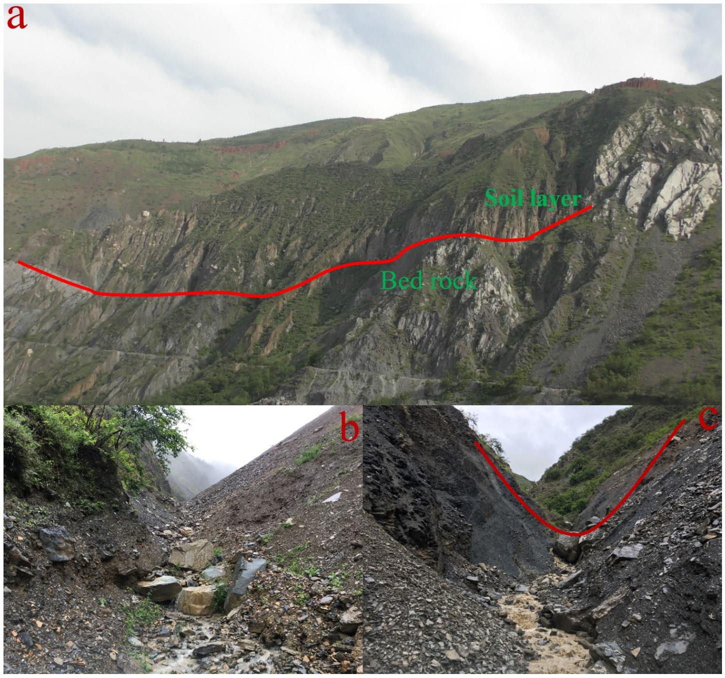

Fig. 3 Loose solid material in JJG

The slopes on both sides of JJG are covered by a loose soil mass tens of meters in thickness [Fig. 3(a)]. Because of intense rainfall, shallow landslides frequently occur on the slopes and provide a large amount of loose solid material for debris flows [Fig. 3(b)]. The steep terrain and large amount of loose solid material in JJG provide suitable conditions for debris flow formation. According to the collected rainfall data, high-intensity or long-duration rainfall can trigger debris flow events (Guo et al., 2013; Zhang et al., 2020). The solid material in JJG originates mainly from shallow landslides, which is consistent with the model assumptions. Therefore, JJG is chosen as the study area to quantitatively examine the effect of AEP on the *ID* threshold curves of debris flows.

3.2 Data for model calculation and validation

◆ Terrain data

https://doi.org/10.5194/hess-2022-57
Preprint. Discussion started: 16 February 2022

DEM data for JJG were provided by the Dongchuan Debris Flow Observation and Research Station. The spatial resolution of the DEM is 0.5 m, and the data were obtained in December 2017 by aerial photogrammetry using an unmanned aerial vehicle. A DEM with a grid size of 10 m was generated from the original terrain data using the resampling tools in ArcGIS, which were used to derive the geometrical parameters of JJG such as slope length, gradient, and river channels.

◆ Data necessary for hydrological simulation

Three main soil types (Table 1) occur in the JJG: dry red soil, red-yellow soil, and gravelly soil. Gravelly soil is widely distributed upstream in JJG and is the main source of solid material for debris flow. The hydrological parameters listed in Table 1 were obtained from the National Soil Database. The grid size of the land use map is 250 m, and its parameters, such as the normalized difference vegetation index, were obtained from the Moderate Resolution Imaging Spectroradiometer database. These data related to hydrological parameters were converted into a map with an accuracy comparable to that of the DEM using the resampling tool in ArcGIS.

Table 1 Soil types and their hydrological parameters

Soil type	θ_s	θ_r	Parameters of curve		f_s (mm/h)
			α	n	
Gravelly soil	0.54017	0.07639	0.02201	1.37785	30.486
Red-yellow soil	0.48519	0.06829	0.02264	1.38146	21.964
Dry red soil	0.48148	0.07640	0.01476	1.47394	10.811

◆ Soil mechanical parameters

Eq. 7 (section 4.3) can be used to determine two soil mechanical parameters, soil cohesion c and internal friction angle φ, by direct shear tests of soil samples from JJG. Most of the solid material for debris flows in JJG originates from gravelly soil; therefore, three groups of soil samples were taken from several typical slopes covered by a gravelly soil mass, and one sample each was taken from the red-yellow and dry red soil. As shown in Table 2, the three samples from

https://doi.org/10.5194/hess-2022-57
Preprint. Discussion started: 16 February 2022

gravelly soils have similar c and φ values; therefore, the average values of the two parameters were calculated to represent the mechanical performance of the gravelly soil mass. The mechanical parameters in Table 2 can be assigned to each grid cell of the DEM according to the distribution of soil types in JJG.

Table 2 Cohesion c and internal friction angle φ of soil samples from JJG

Soil samples	Soil mechanical parameter			
	c (kPa)	φ (deg)	Average c (kPa)	Average φ (deg)
Gravelly soil-1	35.1	36.0	34.5	34.4
Gravelly soil-2	35.9	33.7		
Gravelly soil-3	32.5	33.7		
Red-yellow soil	27.0	36.3	27.0	36.3
Dry red soil	25.9	35.7	25.9	35.7

◆ Historical debris flow and rainfall data

To validate the quantitative relationship between the AEP and the *ID* threshold curves of debris flows, data for 45 debris flow events in JJG and the triggering rainfall processes were collected. Rainfall events must be separated from long-term rainfall sequences to identify the rainfall processes that triggered the 45 debris flow events. The inter-event time (IET) was defined as a measure of the minimum time interval between two consecutive rainfall pulses (Adams et al., 1986). Although the IET strongly affects the start and end times of an event (Bel et al., 2017), there are no standard criteria for rainfall episode separation (Jiang et al., 2021). Peres et al. (2018) noted that the IET depends on whether the rainfall during an IET is smaller than the mean daily potential evapotranspiration (MDPE). Long-term observation of the evaporation in JJG showed that the MDPE in this gully is approximately 4 mm; thus, precipitation of less than 0.5 mm during an IET is considered to indicate the end of a rainfall process.

https://doi.org/10.5194/hess-2022-57
Preprint. Discussion started: 16 February 2022

The AEP was calculated as the weighted sum of rainfall periods before a debris flow (Long et al., 2020) and is expressed as follows:

$$AEP = \sum_{i=1}^{n} K^n R_i \tag{6}$$

where the AEP is the antecedent effective rainfall; *K* is the attenuation coefficient, which is equal to 0.78 according to a field test in JJG (Cui et al., 2003); and *n* is the number of days preceding the debris flow. Table 3 lists the calculated AEP, average rainfall intensity (*I*), and rainfall duration (*D*) of each debris event. The calculated AEP values in the third column of Table 3 are rounded to integers to increase the number of debris flow events corresponding to each AEP. AEP values of 90 and 60 mm are associated with 1 debris flow event each, 8 events have an AEP value of 40 mm, 13 events have an AEP value of 30 mm, 14 events have an AEP value of 20 mm, and 8 events have an AEP value of 15 mm.

Table 3 Historical data of debris flow events and rainfall

Number	Date	AEP	Rounded AEP	Rainfall duration (h)	Intensity (mm/h)
1	2004/7/9	92.60	90	9.30	1.00
2	2001/6/29	59.30	60	4.50	6.70
3	2008/7/5	44.77	40	8.88	1.97
4	2001/7/4	42.50		21.7	1.40
5	2001/7/8	39.80		6.8	3.80
6	2008/8/7	39.73		27.10	1.58
7	2008/6/15	38.87		16.90	1.43
8	2007/7/24	38.35		6.05	2.89
9	1999/8/25	36.20		7.8	3.10
10	2006/7/6	35.20		2.27	10.37
11	1999/7/16	34.00	30	4	11.8

https://doi.org/10.5194/hess-2022-57
Preprint. Discussion started: 16 February 2022

Hydrology and Earth System Sciences
Discussions

12	2008/7/21	33.47		10.43	2.65
13	2000/8/9	31.60		2.3	8.6
14	2008/8/3	31.35		7.25	3.14
15	2010/7/17	30.385		1.00	4.6
16	2001/6/27	30.30		4	13.1
17	2007/9/17	30.15		9.38	2.44
18	2001/8/13	29.80		3.2	5.3
19	1994/6/26	29.00		2	23
20	2008/7/31	28.99		6.93	2.18
21	1999/7/24	28.90		4.8	9.80
22	2001/8/22	28.00		3.50	6.00
23	2008/8/17	26.29		3.75	3.23
24	2006/8/20	24.63	20	3.15	2.32
25	1999/8/10	23.60		14.20	4.30
26	2000/8/8	23.50		5.20	8.50
27	2008/7/1	23.22		9.88	2.60
28	2000/8/29	22.70		6.00	6.20
29	2010/7/6	22.376		10.88	4.18
30	2008/7/11	21.33		1.85	6.43
31	2006/8/15	20.62		3.08	9.79
32	2006/7/5	20.52		2.32	10.53
33	2000/7/15	19.60		26.2	2.90
34	1993/8/29	18.60		6.70	4.60
35	1998/8/2	18.40		3.70	7.30
36	2004/6/26	18.10		3.50	5.00
37	2007/8/24	16.69		28.60	1.77
38	2007/8/11	14.63	15	6.80	1.88
39	2007/7/10	14.40		1.48	7.01

https://doi.org/10.5194/hess-2022-57
Preprint. Discussion started: 16 February 2022

40	2001/6/26	13.40		3.90	11.80
41	2004/7/19	12.60		2.00	9.80
42	1994/6/15	12.50		8.70	6.10
43	1993/8/26	12.10		8.7	3.60
44	2009/8/4	11.90		5.72	9.34
45	2010/9/10	11.51		6.03	5.55

4 Results and Discussion

4.1 *ID* threshold curves of debris flow with different AEP

Fig. 4 shows three sets of *ID* threshold curves for debris flows with AEP values of 20, 60, and 10 mm. All of the axes are given on a logarithmic scale. As shown in Fig. 4(a) (AEP = 20 mm), two *ID* threshold curves corresponding to ρ_{mix} = 1.2 and ρ_{mix} = 2.2 g/cm^3 constitute the boundaries of the rainfall threshold that triggers debris flow in JJG. The *ID* threshold curves in Fig. 4 can be described by a power function; this result is consistent with the shape of the threshold curve obtained by the statistical model, indicating that our model can describe the hydrological process of rainfall-induced debris flow. The *ID* threshold curve corresponding to a density of 2.2 g/cm^3 is located below the curve that corresponds to a density of 1.2 g/cm^3, indicating that debris flows with higher density are more easily triggered in JJG. AEP has a significant qualitative effect on the *ID* threshold curve of a debris flow. Essentially, a large AEP value indicates that the rainfall requirements for rainfall-induced debris flow are low. For *D* = 1 h, the rainfall intensity *I* that can trigger a debris flow with a density of 1.2 g/cm^3 decreases from 26.2 to 16.7 mm/h with increasing AEP. The trend revealed by this calculation result is essentially consistent with the results of field observations in JJG (Cui et al., 2003).

https://doi.org/10.5194/hess-2022-57
Preprint. Discussion started: 16 February 2022

Hydrology and Earth System Sciences
Open Access
Discussions

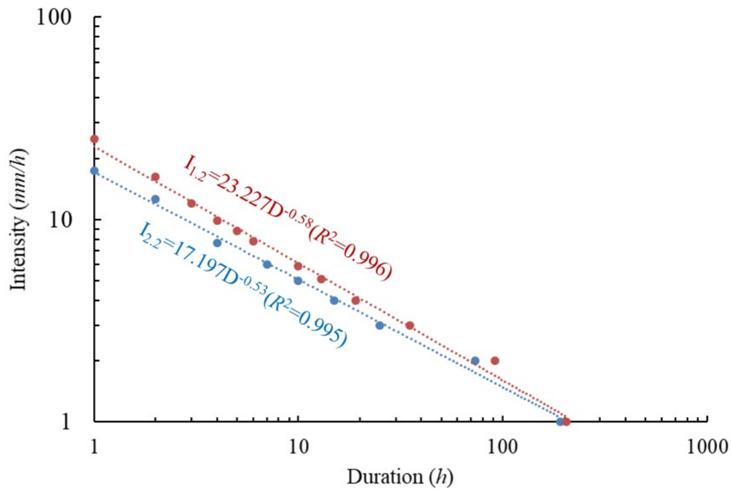

(a) AEP = 20 mm

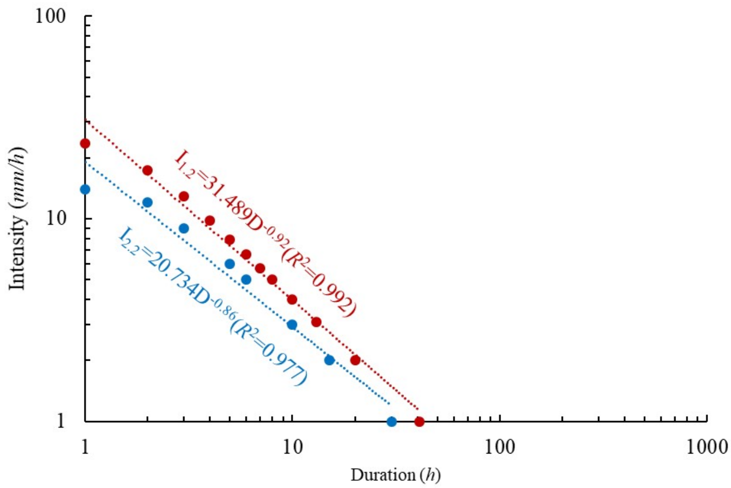

(b) AEP = 60 mm

https://doi.org/10.5194/hess-2022-57
Preprint. Discussion started: 16 February 2022

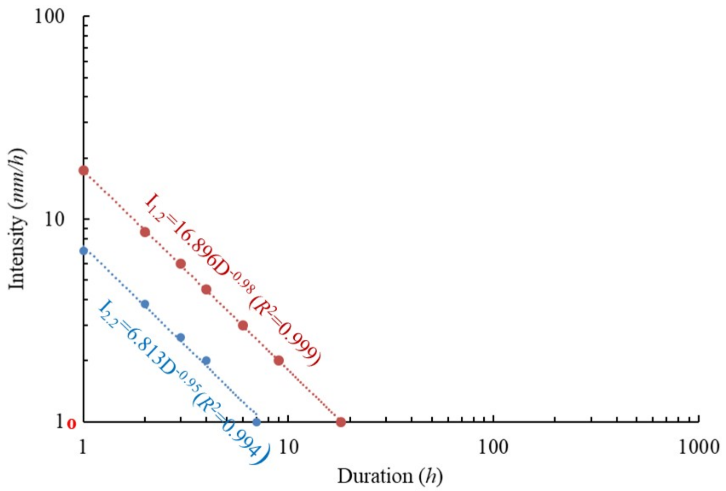

(c) AEP = 100 mm

Fig. 4 *ID* threshold curves of debris flow for different AEP values

In addition, Fig. 4 shows that the distance between the two ID threshold curves becomes larger with increasing AEP, indicating a higher occurrence probability of rainfall-induced debris flow. A database including all the data sets, including [*I*, *D*], the fitted curves, and AEP (Table 4) was used to quantitatively analyze the effect of AEP on the threshold curve.

Table 4 Database of AEP, fitted equations, and [*I*, *D*] data groups

AEP (mm)	Fitted threshold curves of debris flow in JJG	
	1.2 g/cm^3	2.2 g/cm^3
10	$I_{1.2} = 19.851D^{-0.54}$ $D \in [1, 269]$ ($R^2 = 0.991$)	-
15	$I_{1.2} = 21.69D^{-0.55}$ $D \in [1, 236]$ ($R^2 = 0.993$)	$I_{2.2} = 16.10D^{-0.50}$ $D \in [1, 229]$ ($R^2 = 0.995$)
20	$I_{1.2} = 23.227D^{-0.58}$ $D \in [1, 203]$ ($R^2 = 0.996$)	$I_{2.2} = 17.197D^{-0.531}$ $D \in [1, 192]$ ($R^2 = 0.995$)
30	$I_{1.2} = 26.24D^{-0.64}$ $D \in [1, 143]$ ($R^2 = 0.996$)	$I_{2.2} = 18.087D^{-0.57}$ $D \in [1, 132]$ ($R^2 = 0.995$)
40	$I_{1.2} = 40.589D^{-0.78}$ $D \in [1, 103]$ ($R^2 = 0.966$)	$I_{2.2} = 22.154D^{-0.64}$ $D \in [1, 92]$ ($R^2 = 0.984$)
50	$I_{1.2} = 41.263D^{-0.86}$ $D \in [1, 65]$ ($R^2 = 0.981$)	$I_{2.2} = 23.501D^{-0.74}$ $D \in [1, 55]$ ($R^2 = 0.980$)
60	$I_{1.2} = 31.489D^{-0.92}$ $D \in [1, 40]$ ($R^2 = 0.992$)	$I_{2.2} = 20.734D^{-0.86}$ $D \in [1, 30]$ ($R^2 = 0.977$)

https://doi.org/10.5194/hess-2022-57
Preprint. Discussion started: 16 February 2022

Hydrology and Earth System Sciences
Open Access
Discussions

70	$I_{1.2} = 23.049D^{-0.96}$ $D \in [1, 25]$ ($R^2 = 0.9983$)	$I_{2.2} = 13.042D^{-0.93}$ $D \in [1, 15]$ ($R^2 = 0.995$)
80	$I_{1.2} = 18.719D^{-0.98}$ $D \in [1, 20]$ ($R^2 = 0.997$)	$I_{2.2} = 9.960D^{-0.95}$ $D \in [1, 11]$ ($R^2 = 0.999$)
90	$I_{1.2} = 16.991D^{-0.98}$ $D \in [1, 18]$ ($R^2 = 0.999$)	$I_{2.2} = 6.813D^{-0.95}$ $D \in [1, 7]$ ($R^2 = 0.994$)
100	$I_{1.2} = 16.896\mathrm{D}^{-0.98}$ $D \in [1, 18]$ ($R^2 = 0.999$)	$I_{2.2} = 6.813\mathrm{D}^{-0.95}$ $D \in [1, 7]$ ($R^2 = 0.994$)
110	$I_{1.2} = 16.873\mathrm{D}^{-0.98}$ $D \in [1, 16]$ ($R^2 = 0.999$)	$I_{2.2} = 6.755\mathrm{D}^{-0.95}$ $D \in [1, 7]$ ($R^2 = 0.997$)
120	$I_{1.2} = 16.873\mathrm{D}^{-0.98}$ $D \in [1, 16]$ ($R^2 = 0.999$)	$I_{2.2} = 6.755\mathrm{D}^{-0.95}$ $D \in [1, 7]$ ($R^2 = 0.997$)

Note that Dens-ID cannot collect sufficient [I_i, D_i] data for fitting the *ID* threshold curve for a density of 2.2 g/cm^3 and AEP = 10 mm. At this low AEP value, the supply rate of solid material is lower than the runoff rate; thus, it is difficult to trigger a high-density debris flow in JJG. By contrast, for AEP $\geq$ 90 mm, α and β tend to be constant. The AEP can significantly affect the *ID* curves of debris flow in JJG at values of 10 to 90 mm.

4.2 Effects of loose solid material and runoff on debris flow formation

In Dens-ID, the parameters $V_w(t)$ and $V_s(t)$ in Eq. 1 are the process variables for calculating the density of the water-soil mixture. Because the *ID* threshold curves in Fig. 4 are all related to the debris flow density, it is necessary to analyze the relationship between debris flow density and $V_w(t)$ and $V_s(t)$ under different rainfall conditions.

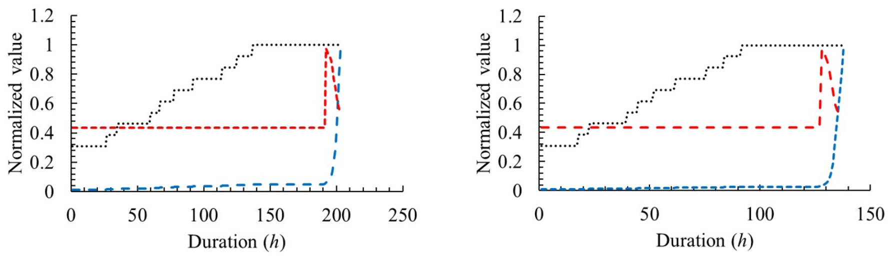

(a) $I = 1$ mm (b) $I = 1.5$ mm

https://doi.org/10.5194/hess-2022-57
Preprint. Discussion started: 16 February 2022

Hydrology and Earth System Sciences
Discussions

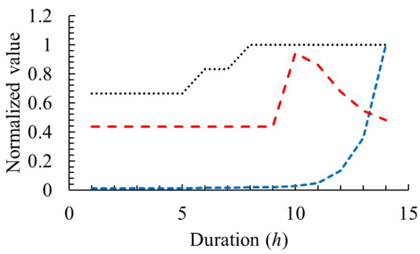

(c) I = 5 mm

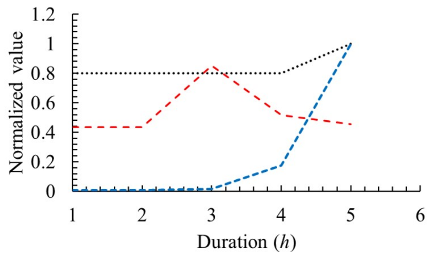

(d) I = 10 mm

Fig. 5 Process graphs of $V_s(t)$, $V_w(t)$, and $\rho_{mix}(t)$ for different rainfall intensity values I and AEP = 20 mm. Black dotted line represents the volume variation of $V_s(t)$, blue dotted line represents the volume variation of $V_w(t)$, and red dotted line represents the density of the water-soil mixture.

Fig. 5 shows process graphs of $V_s(t)$, $V_w(t)$, and $\rho_{mix}(t)$ for different rainfall intensity values I at AEP = 20 mm. Because these three parameters have different magnitudes, they were normalized to better show their dynamic evolution.

The red curve represents the debris flow density for different rainfall intensity values I, which reveals a clear water process (Stage 1), debris flow phase (Stage 2), and hyperconcentrated flow stage (Stage 3). In Stage 1, the runoff rate is lower than the supply rate of solid material (black dotted line) in JJG. During this stage, the runoff in JJG cannot provide hydrodynamic conditions suitable for transporting these loose deposits, and no debris flow occurs. In Stage 2, during continuous hydrological processes such as rainfall infiltration and runoff generation, the total volume of runoff ($V_w(t)$) in JJG increases rapidly, and the blue dotted lines in Fig. 5(a)–(d), which represent the volume variation of $V_w(t)$, all show a sharp increase. Consequently, the hydrodynamic conditions are sufficient for debris flow formation. The rainfall-induced loose solid material and runoff in the channel can be fully coupled, and thus a debris flow can be triggered. In Stage 3, a sudden increase in runoff volume and decrease in the supply rate of loose solid material

https://doi.org/10.5194/hess-2022-57
Preprint. Discussion started: 16 February 2022

cause the debris flow in JJG to quickly become hyperconcentrated. Therefore, the red dotted line in Fig. 5 also shows that debris flows generally begin suddenly but quickly reach Stage 3 because of the rapid increase in runoff.

The black dashed line in Fig. 5 represents the variation of $V_s(t)$. The hydrological conditions represented by AEP = 20 mm induce shallow landslides in JJG before rainfall begins. In the initial stage of the rainfall process, the supply rate of solid material is higher than the runoff rate in JJG; however, as the rainfall process continues, the supply rate is overtaken by the runoff rate, and the total volume stabilizes at a maximum value.

The blue dashed lines in Fig. 5 represent the variation of $V_w(t)$. They all show a sharp increase at a certain time, at which debris flows also occur. Thus, the sudden occurrence of debris flows is caused mainly by increasing runoff. These results indicate that the supply of loose solid material is essential to debris flow formation, but the decisive factor in debris flow occurrence is the sharp increase in runoff.

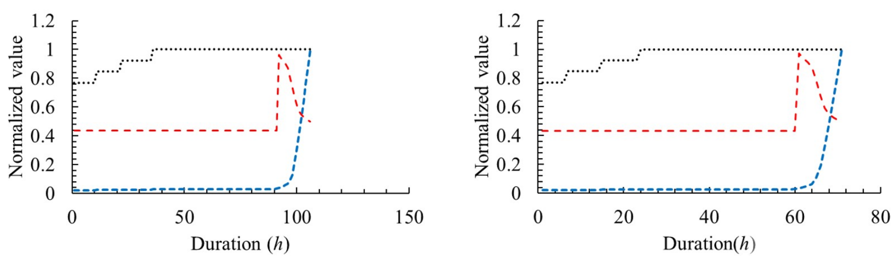

(a) I = 1 mm (b) I = 1.5 mm

https://doi.org/10.5194/hess-2022-57
Preprint. Discussion started: 16 February 2022

Hydrology and Earth System Sciences
Open Access
Discussions

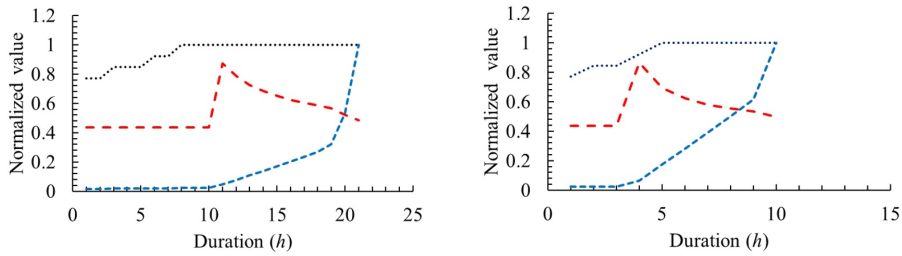

(c) I = 5 mm (d) I = 10 mm

Fig. 6 Process graphs of $V_s(t)$, $V_w(t)$, and $\rho_{mix}(t)$ for different rainfall intensity values I and AEP = 40 mm. Black dotted line represents the volume variation of $V_s(t)$, blue dotted line represents the volume variation of $V_w(t)$, and red dotted line represents the density of the water-soil mixture.

4.3 Quantitative analysis of effects of AEP on α and β

The three *ID* curves from Fig. 4 corresponding to a density of 2.2 g/cm^3 and different AEP values are plotted in Fig. 7 to further examine the variation of the *ID* curves with AEP. The AEP can change the position of the *ID* threshold curve in the *I*–*D* coordinate system, indicating that a higher AEP value shifts the *ID* threshold curve closer to the origin. This tendency is consistent with the general consensus that higher AEP can decrease the triggering rainfall conditions (De Vita et al., 2000; Cui et al., 2003; Bel et al., 2017). Consequently, considering the landslide-dominated solid resource supply in JJG, Dens-ID describes the formation process of rainfall-induced debris flow reasonably well. In addition, compared to the range of rainfall intensity I (Y axis), the rainfall duration D (X axis) changes more dramatically with AEP and can quickly decrease from 192 h (AEP = 20 mm) to 7 h (AEP = 100 mm).

https://doi.org/10.5194/hess-2022-57
Preprint. Discussion started: 16 February 2022

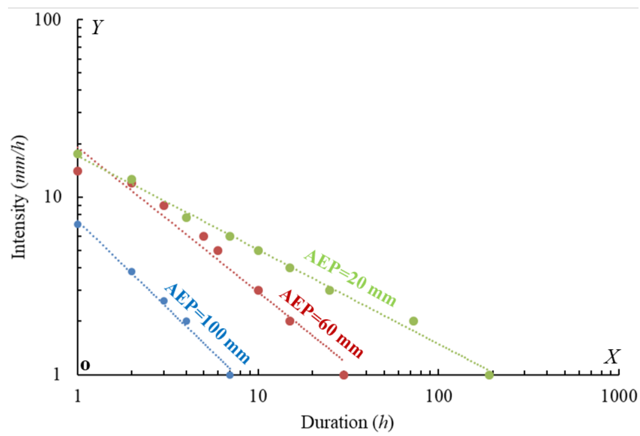

Fig. 7 *ID* curves corresponding to a density of 2.2 g/cm³ and AEP values of 20, 60, and 100 mm

The parameters of the *ID* threshold curve of debris flow, α and β, determine the position of the fitting curve in *I*–*D* coordinates. Therefore, it can be deduced that α and β depend on AEP. In this section, the data sets from Dens-ID are used to derive the functional relationships between AEP and these two parameters. First, it is necessary to clarify the physical meaning of α and β. Under the numerical simulation conditions of this study, the variation interval of the independent variable D in the formula $I = \alpha D^{\beta}$ is [1, D_{max}], and the variation interval of I is [I_{max},1]. According to the formula, when D is equal to 1 h, $I = \alpha$. When $D = 1$, the rainfall duration required to trigger a debris flow is 1 h, and the rainfall intensity I reaches the maximum value, I_{max}. Therefore, the combination of D and I under these conditions represents high-intensity rainfall. According to this analysis, α is numerically equal to the value of I_{max}, and thus this parameter represents the critical rainfall intensity required to trigger a debris flow for $D = 1$ h.

Before the physical meaning of β is discussed, the expression $I = \alpha D^{\beta}$ needs to be written logarithmically, as follows:

$$\log I = \log\alpha + \beta\log D \quad (7)$$

By denoting log$I$ as Y_I, log$D$ as X_D, and logα as B_α, Eq. 7 can be rewritten as follows:

https://doi.org/10.5194/hess-2022-57
Preprint. Discussion started: 16 February 2022

$$Y_I = \beta X_D + B_\alpha \tag{8}$$

X_D and Y_I are related to I and D and are independent variables with ranges of [log1, log(D_{max})] and [log1, log(I_{max})], respectively. The rewritten equation is represented by a linear equation in Figs. 4 and 5, where β is the slope of each line and is less than 0. The main reason that β is less than 0 is a tradeoff between rainfall intensity and rainfall duration in nature, which facilitates the occurrence of debris flow. The absolute value of β represents the deceleration rate of rainfall intensity with increasing rainfall duration, that is, the rate of decrease from I_{max} to 1 mm/h. The α and β values in Table 4 can be classified into two groups according to debris flow density (1.2 or 2.2 g/cm^3). The α and β values in the two groups show similar variation with AEP. Thus, one data group (Table 5) corresponding to a density of 2.2 g/cm^3 was selected to examine the effect of AEP on α and β.

Table 5 Calculated α and β for different AEP values

Fitting parameter	AEP (mm)											
	10	20	30	40	50	60	70	80	90	100	110	120
α	-	17.2	18.1	22.2	23.5	20.7	13.0	9.9	6.8	6.8	6.8	6.8
β	-	−0.53	−0.57	−0.64	−0.74	−0.86	−0.93	−0.95	−0.95	−0.95	−0.95	−0.95

Effect of AEP on α: The effect of AEP on α is described by the following equations, which were fitted using the AEP and α values in Table 5:

$$\begin{cases} \alpha = -0.0078AEP^2 + 0.68AEP + 6.43 & 20 \leq AEP < 90 \\ \alpha = 6.8 & 90 \leq AEP \leq 120 \end{cases} \tag{9}$$

The condition for $\alpha = I_{max}$ is $D = 1$, and the combination of $D = 1$ and α represents a high-intensity, short-duration rainfall process. As shown in Fig. 8, Eq. 9 is used to quantify the rainfall intensity threshold at which this type of rainfall process triggers a debris flow for different AEP

https://doi.org/10.5194/hess-2022-57
Preprint. Discussion started: 16 February 2022

values. In Fig. 8, α (or I_{max}) represents parabolic variation with AEP. Interestingly, α does not always decrease with continuously increasing AEP. When AEP ≤ 50 mm, the α values necessary for triggering a debris flow increase simultaneously with AEP; when AEP > 50 mm, α decreases with increasing AEP, but the decrease does not continue indefinitely with increasing AEP, because for AEP > 90 mm, α is constant at 6.8 mm (Table 5).

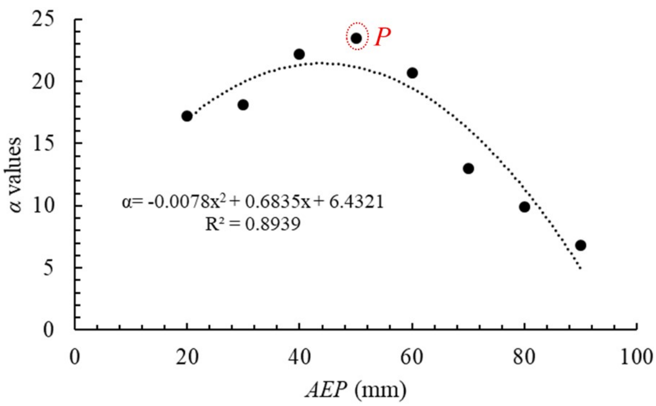

Fig. 8 Function curve describing the relationship between AEP and α

The key variables V_s and V_w are used to explain the quantitative evolution described by Eq. 9. To facilitate the analysis, the V_s and α values calculated by Dens-ID were normalized, and they are plotted versus AEP (AEP–V_s and AEP–α) in Fig. 9. V_s increases continuously for AEP < 50 mm, at which it reaches a maximum. As V_s increases with increasing AEP, a larger volume value of runoff (V_w) is required to bring the debris flow density (ρ_{mix}) to a fixed value of 2.2 or 1.2 g/cm^3, which requires stronger hydrodynamic conditions, and thus a higher hourly rainfall intensity. Before point P_1 in Fig. 9, the rainfall intensity (or α) at which a debris flow occurs for D = 1 is positively correlated with AEP. Although AEP no longer contributes to the variation of V_s after AEP reaches 50 mm, the soil water content can still increase with continuously increasing AEP, reducing the surface infiltration rate and increasing the runoff volume generated from rainfall.

https://doi.org/10.5194/hess-2022-57
Preprint. Discussion started: 16 February 2022

Under these hydrological conditions, the rainfall intensity I_{max} (or α) required to trigger a debris flow with a fixed density value decreases gradually; thus, α is negatively correlated with AEP. When AEP exceeds 90 mm (P_2 in Fig. 9), α stops gradually decreasing and remains constant, indicating that at AEP = 90 mm, the loose solid material in JJG become saturated. Under these hydrological conditions, α has a constant value of 6.8 mm and does not change with AEP. Therefore, for the two inflection points P_1 and P_2 in Fig. 9, AEP is the external driving factor and operates through the entire process of debris flow formation in JJG, whereas the limiting conditions, maximum V_s and constant saturated soil water content (θ_s), are the two intrinsic factors.

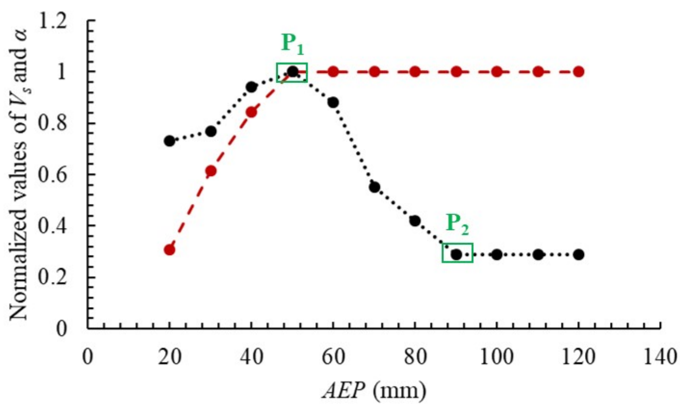

Fig. 9 AEP–α curve (black dashed line) and AEP–V_s curve (red dashed line)

Effect of AEP on β: The effect of AEP on β is described by the following equations, which were fitted using the AEP and β values in Table 5.

$$\begin{cases} \beta = -0.0079AEP - 0.35 & 20 \le AEP < 90 \\ \beta = -0.95 & 90 \le AEP \le 120 \end{cases} \quad (10)$$

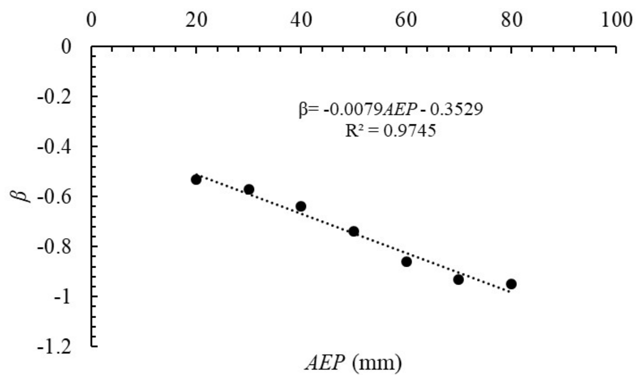

Fig. 10 Function curve describing the relationship between AEP and β for AEP values ranging from 20 to 90 mm

Eq. 10 and Fig. 10 show that as AEP increases from 20 to 90 mm, β decreases linearly. When AEP exceeds 90 mm, β becomes a constant with a value of −0.95. These results, in combination with Eq. 9, reveal that α and β in the *ID* threshold equation are constant when AEP exceeds 90 mm. This result further shows that there is an interval in which AEP affects the *ID* threshold curve of debris flow in JJG, specifically, AEP $\in$ [20,90].

4.4 Validation of quantitative relationship

Using the historical rainfall data in Table 3, four *ID* threshold curves for different AEP values were fitted, as shown Fig. 11. The green dotted line represents AEP = 15 mm, and the fitted equation is $I = 11.99D^{-0.45}$. The red dotted line represents AEP = 20 mm ($I = 10.58D^{-0.44}$). The black dotted line represents AEP = 30 mm ($I = 13.16D^{-0.60}$). The orange dotted line represents AEP = 50 mm ($I = 15.25D^{-0.78}$). These lines differ when D is larger than 3. For $D > 3$, the ID threshold curve appears lower in the *I–D* coordinate system with increasing AEP, indicating that lower rainfall conditions will trigger debris flow. This tendency is consistent with the simulated results in Fig. 7, further demonstrating that Dens-ID may be able to describe the formation process of rainfall-induced debris flow.

https://doi.org/10.5194/hess-2022-57
Preprint. Discussion started: 16 February 2022

Hydrology and Earth System Sciences
Open Access
Discussions

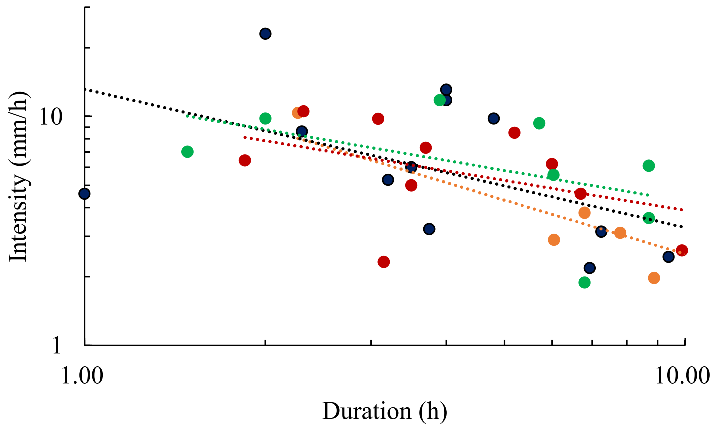

Fig. 11 Historical-data-based *ID* curves for different AEP values. Green, red, black, and orange symbols and lines represent AEP values of 15, 20, 30, and 50, respectively.

The curves fitted using historical rainfall data and Dens-ID for the same AEP were drawn in separate graphs, where each graph corresponds to a different AEP value between 15 and 90 mm. As shown in Table 2, only one debris flow event each was collected from the observation station for AEP values of 60 and 90 mm. In Fig. 12(e) and (f), the single points at which the I and D data in Table 3 coincide with the model-derived curves are indicated. These points are located between the threshold curves, which are isodensity curves corresponding to debris flow densities of 2.2 and 1.2 g/cm^3. Any combination of I and D between these two isodensity curves indicates that these rainfall conditions can trigger a debris flow. Because the closed area formed by the two curves covers historical data on rainfall that triggered a debris flow event, the curves derived by Dens-ID are at reasonable positions in I–D coordinates (that is, the α and β values that determine the position of $I = \alpha D^{\beta}$ in I–D coordinates are reasonable). Therefore, the α and β values of the Dens-ID-derived threshold curves corresponding to AEP values of 60 and 90 mm can be used to analyze the relationship between AEP and α and β.

Forty-three debris flow events corresponding to AEP values of 15, 20, 30, and 40 mm are

https://doi.org/10.5194/hess-2022-57
Preprint. Discussion started: 16 February 2022

Hydrology and Earth System Sciences
Open Access
EGU
Discussions

plotted in Fig. 12(a)–(d). Four *ID* threshold curves (black dashed lines) corresponding to these AEP values were fitted using the rainfall data associated with each event. In each panel, the red and blue lines are *ID* threshold curves fitted by Dens-ID for debris flow densities of 1.2 g/cm^3 (the upper boundary for identifying debris flow formation) and 2.2 g/cm^3 (the lower boundary), respectively (Zhang et al., 2020). If a data point representing (I, D) is above the black dashed or blue line, these rainfall conditions may trigger debris flows (Cain, 1980; Zhang et al., 2020). Although the black dashed and blue lines were fitted by different methods, both are used as lower limits for identifying debris flow formation. By using the black dashed line as a reference, the blue line can be calibrated according to its deviation from the black dashed line for each AEP value; then the errors of the equations describing the relationships between AEP and α and β (Eqs. 9 and 10, respectively) can be evaluated.

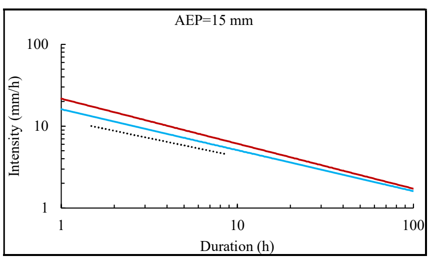

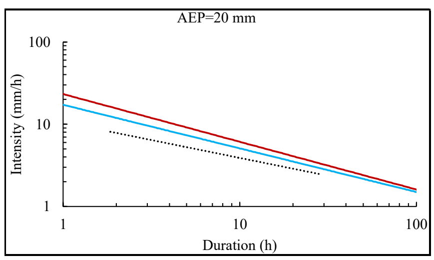

(a) AEP = 15 mm (b) AEP = 20 mm

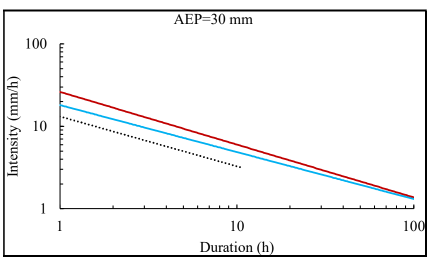

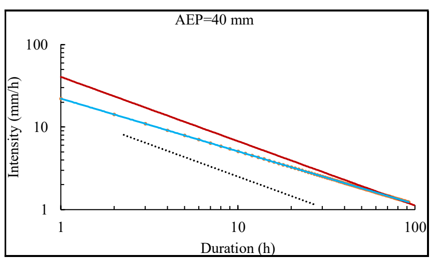

(c) AEP = 30 mm (d) AEP = 30 mm

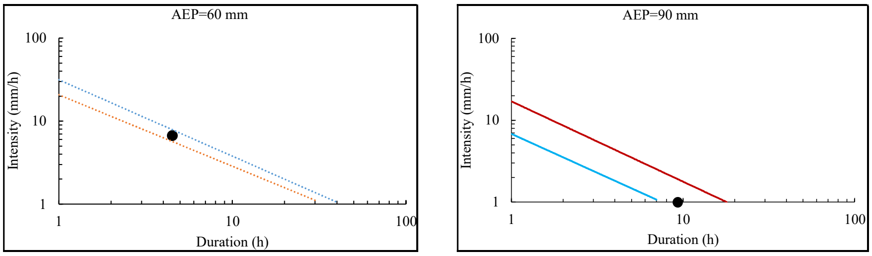

(e) AEP = 60 mm (f) AEP = 90 mm

Fig. 12 *ID* threshold curves fitted using historical data in Table 3 (black dashed line) and Dens-ID (blue and red lines)

As shown in Table 6, the errors of α for AEP values of 40, 30, 20, and 15 mm are 39.1%, 50.1%, 27.1%, and 35.1%, respectively, and the average error is approximately 37.85%. The errors of β for AEP values of 40, 30, 20, and 15 mm are 14.6%, 21.7%, 2.30%, and 5.80%, respectively, and the average error is approximately 11.10%. According to the physical meaning of α and β, the error of Eq. 9 (approximately 37.85%) indicates that Dens-ID overestimates the triggering rainfall intensity (I_{max}) for D = 1. Additionally, the calculated β values, which represent the deceleration rate of rainfall intensity with increasing rainfall duration, have a smaller error than the α values.

Table 6 Error calibration using historical data

AEP (mm)	Fitted by historical data		Fitted by Dens-ID		Error (%)	
	α	β	α	β	α	β
40	15.2	−0.78	21.15	−0.666	39.1	14.6
30	13.2	−0.6	19.81	−0.587	50.1	21.7
20	13.3	−0.52	16.91	−0.508	27.1	2.3
15	12	−0.45	14.875	−0.4685	35.1	5.8

The threshold curves fitted using historical rainfall data are below the Dens-ID fitting curves in *I*–

D coordinates for the following reasons. (1) The process of debris flow formation in the gully is extremely complex, but Dens-ID cannot fully describe this process because of necessary simplifications in the code. Consequently, the simulated data may differ from the observed rainfall data, especially the triggering rainfall intensity (I_{max} or α) for $D = 1$. (2) According to Zhang et al. (2020, 2021), Dens-ID is sensitive to input parameters such as rainfall, hydrology parameters, and soil mechanical parameters, and it is most sensitive to soil cohesion. Unavoidable uncertainties in many input parameters for the physical model can significantly affect the calculation results of Dens-ID (Raia et al., 2014; Zhang et al., 2018; Jacobs et al., 2020). (3) Local heavy rainfall in JJG is the main trigger for debris flow. The historical rainfall data in Table 3 were obtained at the rainfall station represented by a red circle in Fig. 2, which is approximately 2 km from Menqian Gully. Because of this spatial deviation, the rain gauge may be unable to detect the center of rainstorms, and thus the measured rainfall data may be smaller than the actual values.

5 Conclusions

Rainfall simulations using Dens-ID were employed to construct a database of *ID* threshold curves under different AEP conditions, and this database was used to thoroughly examine the quantitative effect of AEP on the *ID* threshold curves. The following conclusions are drawn.

(1) The *ID* threshold curve obtained using Dens-ID can be expressed by a power function, and the R^2 values of the fitted power functions are all larger than 96%. The fitted curves from our model are all consistent in shape with the threshold curve obtained from the statistical model, indicating that the model can reflect the hydrological process of rainfall-induced debris flow with high reliability.

(2) The relationships between AEP and the parameters α and β can be described by

https://doi.org/10.5194/hess-2022-57
Preprint. Discussion started: 16 February 2022

functions that were verified using the *ID* curves fitted using historical rainfall data for JJG. The errors of the relationships between AEP and α and β are approximately 37.85% and 11.10%, respectively. That is, Dens-ID overestimates the effects of AEP on α and β compared to those indicated by historical rainfall data. This result can be attributed to limitations on the ability of Dens-ID to describe debris flow formation, the uncertainty of the input parameters of Dens-ID, and the suitability of rain gauge data for detecting rainstorm centers.

(3) The two derived equations can clarify the variation of debris flow *ID* curves with AEP. The conventional *ID* threshold curve remains the same regardless of AEP once it is determined. However, the AEP can significantly affect the determination of the *ID* curve. The effects of AEP on α and β cause the originally static *ID* curve to become a variable threshold in the *I–D* coordinate system. Consequently, the *ID* curves fully reflect the effects of AEP when they are used to predict debris flow. Our study may improve the prediction precision of *ID* curves.

Acknowledgement:

This work was supported by the National Key Research and Development Program of China (2018YFC1505503), Project of the Department of Science and Technology of Sichuan Province (No. 2021YFG0258), National Natural Science Foundation of China (No. 42001100).

References

Adams, B., Fraser, H., Howard, C., Hanafy, M. (1986). Meteorological data analysis for drainage system design. J. Environ. Eng. 112

Baum, R.L., Savage, W.Z., and Godt, J.W. (2002). TRIGRS-a FORTRAN program for transient rainfall infiltration and grid-based regional slope stability analysis, Virginia, US Geological Survey Open file report, 02-424.

https://doi.org/10.5194/hess-2022-57
Preprint. Discussion started: 16 February 2022

Hydrology and Earth System Sciences
Open Access
Discussions

Baum, R.L., Savage, W.Z., and Godt, J.W. (2008). TRIGRS-a FORTRAN program for transient rainfall infiltration and grid-based regional slope stability analysis, Virginia, US Geological Survey Open file report, 2008-1159.

Bel, C., Liébault, F., Navratil O., Eckert N., Bellot H., Fontaine, F., Laigle, D. (2017). Rainfall control of debris-flow triggering in the Réal Torrent, Southern French Prealphs, 291, 17-32.

Berti, M., Bernard, M., Gregoretti, C., Simoni, A. (2020). Physical interpretation of rainfall thresholds for runoff-generated debris flows. Journal of Geophysical Research-Earth Surface, 125, e2019JF005513.

Berti, M., Simoni, A. (2005). Experimental evidences and numerical modelling of debris flow initiated by channel runoff. Landslides 3, 171–182

Caine, N. (1980). The rainfall intensity-duration control of shallow landslides and debris flows. Geogr. Ann. Ser. A Phys. Geogr., 62, 23–27.

Cannon, S., Gartner, J., Wilson, R., Bowers, J., Laber, J. (2008). Storm rainfall conditions for floods and debris flows from recently burned areas in southwestern Colorado and southern California. Geomorphology, 96, 250-269.

Castillo, V.M., Gómez-Plaza, A., Martínez-Mena, M. (2003). The role of antecedent soil water content in the runoff response of semiarid catchments: a simulation approach. J. Hydrol., 284 (1–4), 114–130.

Chen, C.Y., Chen, T.C., Yu, F.C., Yu, W.H., Tseng, C.C. (2005). Rainfall duration and debris-flow initiated studies for real-time monitoring. Environ Geol., 47, 715–724.

Chen, C.W., Oguchi, T., Chen, H., Lin, G.W., (2018). Estimation of the antecedent rainfall period for mass movements in Taiwan. Environ. Ear. Sci., 77, 184.

https://doi.org/10.5194/hess-2022-57
Preprint. Discussion started: 16 February 2022

Chmiel, M., Walter, F., Wenner, M., Zhang, Z., Mcardell, B.W., Hibert, C. (2020). Machine learning improves debris flow warning. Geophysical Research Letter, 48, e2020GL090874.

Church, M., Jakob, M. (2020). What is a debris flood? Water Resour. Res., 56, e2020WR027144.

Coe, J.A., Kinner, D.A., Godt, J.W. (2008). Initiation conditions for debris flows generated by runoff at Chalk Cliffs, central Colorado. Geomorphology, 3, 270–297.

Crosta, G.B., Frattini, P. (2003). Distributed modeling of shallow landslides triggered by intense rainfall. Nat. Hazards Earth Syst. Sci., 3, 81–93.

Cui, P., Yang, K., Chen, J. (2003). Relationship between occurrence of debris flow and antecedent precipitation: taking the Jiangjia Gully as an example, China. J. Soil Water Conserv., 1, 11-15 (in Chinese).

Dahal, R.K., Hasegawa, S. (2008). Representative rainfall thresholds for landslides in the Nepal Himalaya. Geomorphology, 100, 429-443.

Gabet, E.J., Mudd, S.M. (2006). The mobilization of debris flows from shallow landslides. Geomorphology, 1, 207–218.

Giannecchini, R., Galanti, Y., D'Amato, A. G. (2012). Critical rainfall thresholds for triggering shallow landslides in the Serchio River valley (Tuscany, Italy). Nat. Hazards Earth Syst. Sci., 12, 829-842.

Glade, T., Crozier, M.J., Smith, P. (2000). Applying probability determination to refine landslide-triggering rainfall thresholds using an empirical "Antecedent Daily Rainfall Model". Pure Appl. Geophys., 157, 1059–1079.

Guo, X.J., Cui, P., Li, Y. (2013). Debris flow warning threshold based on antecedent rainfall: a case study in Jiangjia Ravine, Yunnan, China. J. Mount. Sci., 10, 305-314.

https://doi.org/10.5194/hess-2022-57
Preprint. Discussion started: 16 February 2022

Guzzetti, F., Peruccacci, S., Rossi, M., Strak, C.P. (2008). The rainfall intensity–duration control of shallow landslides and debris flows: an update. Landslides, 5, 3-17.

Hasnawir, Kubota, T. (2008). Analysis of critical value of rainfall to induce landslides and debris-flow in Mt. Bawakaraeng Caldera, South Sulawesi, Indonesia. J. Fac. Agric. Kyushu Univ., 53, 523-527.

Hirschberg, J., Badoux, A., McArdell, B.W., Leonarduzzi, E., Molnar, P. (2021). Evaluating methods for debris-flow prediction based on rainfall in an Alpine catchment. Nat. Hazards Earth Syst. Sci. 21, 2773-2789.

Iverson, R. M., Reid, M. E., LaHusen, R. G. (1997). Debris flow mobilization from landslides. Annu. Rev. Earth Planet, 25, 85-138.

Jacobs L., Kervyn, M., Reichenbach, P., Rossi, M., Marchesini, I., Alvioli, M., Dewitte, O., 2020. Regional susceptibility assessments with heterogeneous landslide information: Slope unit- Vs. pixel-based approach. Geomorphology, 356: 107084.

Jiang, Z.Y., Fan, X.M., Subramanian, S.S., Yang, F., Tang, R., Xu, Q., Huang, R.Q. (2021). Probabilistic rainfall thresholds for debris flows occurred after the Wenchuan earthquake using a Bayesian technique. Eng. Geo., 280, 105965.

Jones, R., Thomas, R.E., Peakall, J., Manville, V. (2017). Rainfall-runoff properties of tephra: Simulated effects of grain-size and antecedent rainfall. Geomorphology, 282, 39-51.

Khan, Y.A., Lateh, H., Baten, M.A., Kamil, A.A. (2012). Critical antecedent rainfall conditions for shallow landslides in Chittagong City of Bangladesh. Environ. Earth Sci., 67, 97-106.

Kim, S.W., Chun, K.W., Kim, M., Catani, F., Choi, B., Seo, J. (2021). Effect of antecedent rainfall conditions and their variations on shallow landslide-triggering rainfall thresholds in South

https://doi.org/10.5194/hess-2022-57
Preprint. Discussion started: 16 February 2022

Korea. Landslides, 18, 569-582.

Kim, S.K., Hong, W.P., Kim, Y.M. (1991). Prediction of rainfall-triggered landslides in Korea. In: Bell DH (ed) Landslides, Proceedings of the 6th International Symposium on Landslides, vol 2. Balkema, Rotterdam, pp 989-994.

Le Bissonnais, Y., Renaux, B., Delouche, H. (1995). Interactions between soil properties and moisture content in crust formation, runoff and interrill erosion from tilled loess soils. Catena, 25(1), 33-46.

Lehmann, P., Or, D. (2012) Hydromechanical triggering of landslides: From progressive local failures to mass release. Water Resour. Res., 48, W03535.

Liu, D.L., Zhang, S.J., Yang, H.J., Zhao, L.Q., Jiang, Y.H., Tang, D., Leng, X.P. (2016). Application and analysis of debris-flow early warning system in Wenchuan earthquake-affected area. Nat. Hazards Earth Syst. Sci., 16, 483-496.

Long, K., Zhang, S.J., Wei, F.Q., Hu, K.H., Zhang, Q., Luo, Y. (2020). A hydrology-process based method for correlating debris flow density to rainfall parameters and its application on debris flow prediction. Journal of Hydrology, 589, 125124.

Luk, S.H. (1985). Effect of antecedent soil moisture content on rainwash erosion. Catena, 12, (2–3), 129–139.

Marno, P., Peres, D.J., Cancelliere, A., Greco, R., Bogaard, T.A. (2020). Soil moisture information can improve shallow landslide forecasting using the hydrometeorological threshold approach. Landslides, 17, 2041-2054.

Marra, F., Destro, E., Nikolopoulos, E.I., Zoccatelli, D., Creutin, J.D., Guzzetti, F., Borga, M. (2017). Impact of rainfall spatial aggregation on the identification of debris flow occurrence

https://doi.org/10.5194/hess-2022-57
Preprint. Discussion started: 16 February 2022

Hydrology and Earth System Sciences
Open Access
Discussions

thresholds. Hydrol. Earth Syst. Sci., 21, 4525-4532.

Minder, J.R., Roe, G.H., Montgomery, D.R. (2009). Spatial patterns of rainfall and shallow landslide susceptibility. Water Resour. Res., 45, W04419.

Oorthuis, R., Hurlimann, M., Abanco, C., Moya, J., Carleo, L. (2021). Monitoring of rainfall and soil moisture at the Rebaixader catchment (Central Pyrenees). Environmental & Engineering Geoscience, 27(2), 221-229.

Papa, M.N., Medina, V., Ciervo, F., Bateman, A. (2013). Derivation of critical rainfall thresholds for shallow landslides as a tool for debris flow early warning systems. Hydrol. Earth Syst. Sci. 17, 4095-4107.

Peres, D.J., Cancelliere, A. (2014). Derivation and evaluation of landslide-triggering thresholds by a Monte Carlo approach. Hydrol. Earth Syst. Sci., 18, 4913-4931.

Raia, S., Alvioli, M., Rossi, M., Baum, R.L., Godt, J.W., Guzzetti, F., 2014. Improving predictive power of physically based rainfall-induced shallow landslide models: a probabilistic approach, Geosci. Model Dev., 7, 495-514.

Richards, L.A., 1931. Capillary condition of liquids in porous mediums. Physics 1, 318–333.

Ruette, J.V., Lehmann, P., Or, D. (2014) Effects of rainfall spatial variability and intermittency on shallow landslide triggering patterns at a catchment scale. Water Resour. Res., 50, 7780-7799.

Segoni, S., Piciullo, L., Gariano, S.L. (2018). A review of the recent literature on rainfall thresholds for landslide occurrence. Landslides, 15, 1483-1501.

Theule, J.I., Liébault, F., Laigle, D., Loye, A., Jaboyedoff, M. (2015). Channel scour and fill by debris flows and bedload transport. Geomorphology, 243, 92-105.

Tisdall, A. (1951). Antecedent soil moisture and its relation to infiltration. Aust. J. Agric. Res., 2

(3), 342–348.

Yang, H.J., Wei, F.Q., Ma, Z.F., Gao, H.Y., Su, P.C., Zhang, S.J. (2020). Rainfall threshold for landslide activity in Dazhou, southwest China. Landslides, 17, 61-77.

Zhang, S.J., Jiang, Y.H., Yang, H.J., Liu, D.L. (2015). An hydrology-process based method for antecedent effect rainfall determination in debris flow forecasting. Adv. Water Sci., 26, 35-43. (In Chinese)

Zhang, S.J., Ma, Z.G., Li, Y.J., Hu, K.H., Zhang, Q., Li, L. (2021). A grid-based physical model to analyze the stability of slope unit. Geomorphology, 391, 107887.

Zhang, S.J., Wei, F.Q., Liu, D.L., Yang, H.J., Jiang, Y.H. (2014b). A regional-scale method of forecasting debris flow events based on water-soil coupling mechanism. J. Mount. Sci., 6, 1531-1542.

Zhang, S.J., Xu, C.X., Wei, F.Q., Hu, K.H., Xu, H., Zhao, L.Q., Zhang, G.P. (2020). A physics-based model to derive rainfall intensity-duration threshold for debris flow. Geomorphology, 351, 106930.

Zhang, S.J., Yang, H.J., Wei, F.Q., Jiang, Y.H., Liu, D.L. (2014a). A model of debris flow forecast based on the water-soil coupling mechanism. J. Earth Sci., 4, 757-763.

Zhang, S.J., Zhao, L.Q., Delgado Tellez, R., Bao, H.J. (2018). A physics-based probabilistic forecasting model for rainfall-induced shallow landslides at regional scale. Nat. Hazards Earth Syst. Sci., 18, 969-982.

Zhao, B.R., Dai, Q., Han, D.W., Dai, H.C., Mao, J.Q., Mao, J.Q., Zhuo, L. (2019). Probabilistic thresholds for landslides warning by integrating soil moisture conditions with rainfall thresholds. Journal of Hydrology, 574, 276-287.